Discovery of *trans*-HSSSH

M. Liedtke, A. H. Saleck, K. M. T. Yamada, and G. Winnewisser*

I. Physikalisches Institut, Universität zu Köln, D-50937 Köln 41, Germany

D. Cremer* and E. Kraka

Theoretical Chemistry, University of Göteborg, Kemigården 3, S-41296 Göteborg, Sweden

A. Dolgner and J. Hahn

Institut für Anorganische Chemie, Universität zu Köln, D-50939 Köln 41, Germany

S. Dobos

Institute of Isotopes, Hungarian Academy of Sciences, H-1525 Budapest, Hungary

*Received: March 30, 1993; In Final Form: July 29, 1993**

trans(+synclinal(sc),+synclinal(sc))-H_2S_3 (**1**) has been detected and characterized in a mixture of **1** and *cis*(+sc,–sc)-H_2S_3 (**2**) employing millimeter wave and infrared Fourier transform spectroscopy together with ab initio calculations. In the millimeter wave spectrum the identification has been confirmed by the detection of several *Q*-branches with *J* structures that exhibit the typical intensity alternation of 3:1 for all those lines for which the asymmetry splitting can be observed. The intensity alternation is characteristic for asymmetric top rotors with C_2-rotational symmetry, which for **1** is aligned to the *b*-inertial axis. The rotational constants (MHz) are as follows: **1** (trans), A = 14098.89744 (42); B = 2750.15137 (15); C = 2371.69779 (14); **2** (cis), A = 14103.20962 (25); B = 2752.75945 (11); C = 2373.86989 (12). Gas-phase infrared spectra of H_2S_3 have been recorded at medium resolution Fourier transform spectroscopy. Both MP2/TZ+P and QCISD/TZ+P calculations suggest that **1** is 0.25 kcal/mol (87 cm^{-1}) more stable than **2**, which is in agreement with experimental results. The stability of **1** and **2** results from anomeric delocalization of sulfur lone pair electrons where the energy difference between the two conformations is caused by a more favorable alignment of SH bond dipole vectors in **1**. The calculated barrier to internal rotation from **1** to **2** is 8.3 kcal/mol (2900 cm^{-1}). Calculated dipole moments and infrared spectra agree with experimental results.

1. Introduction

The understanding of stereoelectronic effects is one of the basic prerequisites for the prediction of molecular conformations and molecular reactivity, in particular in those cases in which heteroatoms are involved. Heteroatoms such as oxygen and sulfur add to the stability of a molecule provided a conformation is adopted that allows anomeric delocalization of lone pair electrons to σ^* MOs. In molecules that are predominantly made up of heteroatoms, stereoelectronic effects of lone pair electrons accumulate and lead to exceptional conformational behavior and exceptional reactivity. Well-known examples are polysulfanes, which by anomeric delocalization of their lone pair electrons should form helices as shown in Chart I. The first step in the folding of a sulfur chain to a helix should be found for hydrogen trisulfide and, therefore, an experimental investigation of its conformational behavior is desirable.

Hydrogen trisulfide, H_2S_3, is like hydrogen trioxide, H_2O_3, a geminal double rotor that can adopt an infinite number of different conformations by (coupled or uncoupled) rotation at the two SS bonds. The conformational potential of H_2O_3 is rather accurately known from ab initio calculations[1] and, therefore, one knows that of the seven conformers **1**–**7** shown in Chart II the two forms **1** and **2** occupy global and local minima of the conformational surface spanned by the two rotational angles θ_1 and θ_2. The forms **3**, **4**, and **5** occupy global and local maxima and forms **6** and **7** saddle points. Furthermore, it is known that the stability of the (+sc, +sc) and (+sc, –sc) forms **1** and **2** results from the fact that electron lone pair-electron lone pair repulsion is minimal and anomeric stabilization is optimal.[1] As can be seen from Charts I and II conformation **1** leads to a helix form while conformation **2** leads to the acyclic analog of the crown form of an *N*-membered oxygen-ring (envelope for N = 5, chair for N = 6, chair–chair for N = 7, crown form for N = 8, etc.). In the case of H_2O_3, the formation of a helix form is energetically clearly more favorable than that of a closed crown form.[1]

In view of the electronic relationship between sulfur and oxygen it is reasonable to expect that similar electronic effects dominate the conformational behavior of H_2S_3. Therefore, the most stable H_2S_3 conformation should be the C_2-symmetrical (+sc,+sc) form **1** followed by the C_s-symmetrical (+sc,–sc) form **2**, for reasons of simplicity henceforth called *trans* and *cis* forms.[2] Preliminary Hartree–Fock calculations carried out with a DZ+P basis[3] confirmed the existence of two stable conformers but also showed that contrary to H_2O_3 the energy difference between the *trans* and *cis* forms is at 0.3 kcal/mol, so small that on the basis of these calculations alone a reliable prediction of the more stable H_2S_3 conformation and a preference for helix or crown formation is not possible.

First experimental evidence of gas-phase H_2S_3 has been provided through its rotational spectrum recorded in the millimeter-wave region.[4] On the basis of convincing spectroscopic evidence the strongest lines of the measured spectra have been assigned to the *cis* form **2**.[5] However, infrared and Raman spectroscopy of H_2S_3 in solution[6] led to results that were explained by the existence of a *trans* conformer **1**. More recent work has added to the evidence that suggests the existence of **1** in the gas phase.[7] However, up to this point an unequivocal proof of the *trans* form in the gas phase and a clarification of the relative stabilities of *cis* and *trans* forms have not been given.

* Abstract published in *Advance ACS Abstracts*, September 15, 1993.

0022-3654/93/2097-11204$04.00/0 © 1993 American Chemical Society

CHART I

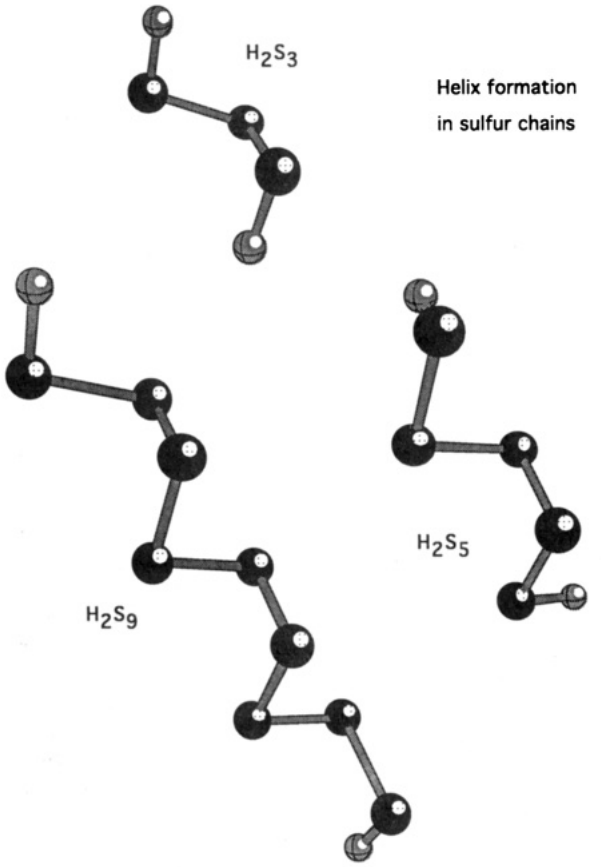

CHART II

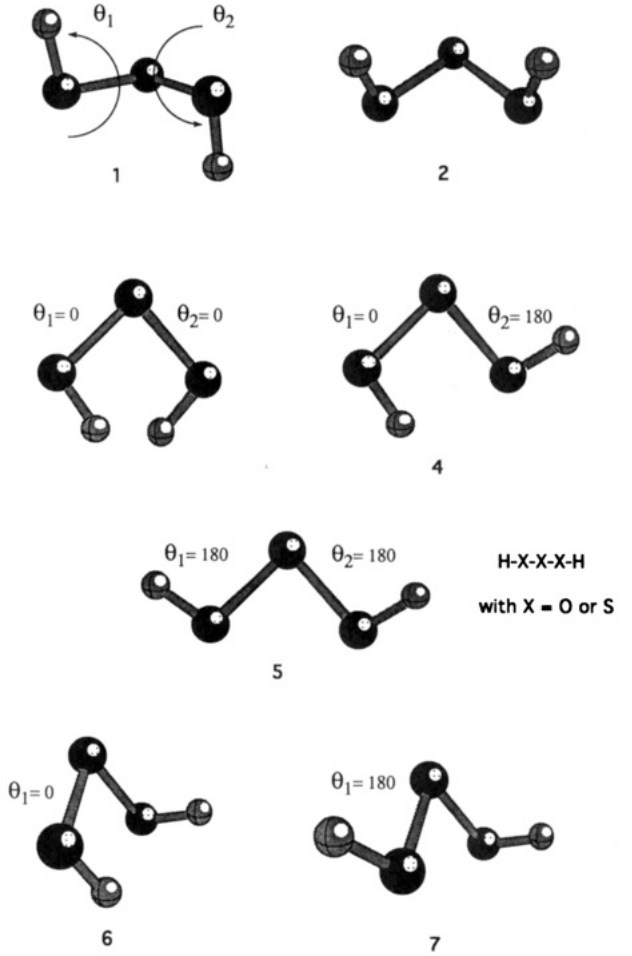

In this work we report the detection of high-J Q-branch transitions in the millimeter wave spectrum of H_2S_3 that provide unequivocal evidence of the existence of the *trans* form **1**. In addition, we compare the results of high level ab initio calculations leading to reliable data on relative stabilities, rotational barriers, dipole moments, and infrared spectra of both the *trans* and *cis* forms with our experimental results.

2. Experimental Section

The pure rotational spectra were measured by using the millimeter-wave spectrometer described by Liedtke and co-workers.[8] Several Gunn oscillators and two backward wave oscillators (Carcinotrons, Thomson-CSF) were employed to deliver the millimeter-wave radiation to the computer-controlled millimeter-wave spectrometer. The spectra were recorded in second derivative form with source frequency modulation in the range from 60 to 300 GHz. The cell (4.4 m long Pyrex tube of 10 cm diameter with PTFE windows) was conditioned by introducing HCl gas with a pressure of 0.1 mbar prior to the measurements. The spectra were obtained at pressures between 20 and 40 μbar.

The infrared spectrum of H_2S_3 has been measured for the first time in the gas phase with a medium resolution infrared FT spectrometer (Bruker IFS48) with a resolution of 0.5 cm^{-1} in the range from 400 to 4000 cm^{-1}. The spectrum was recorded in a flow using Ar as the carrier gas in order to avoid rapid decomposition of the sample at the slightly elevated pressure required for infrared measurements. The Ar gas was introduced into a sample tube of H_2S_3, the temperature of which was kept at 3 °C, and the vapor of H_2S_3 was transported into the cell by the Ar flow with a total pressure of a few mbar. The cell used is 18 cm long made of Pyrex with KBr windows.

The H_2S_3 sample was prepared by utilizing an improved protolysis procedure from silylsulfane $(MePh_2Si)_2S_3$ with excess trifluoroacetic acid, CF_3COOH (molar ratio = 1:5).

$$(MePh_2Si)_2S_3 + 2CF_3COOH \xrightarrow{H_2O\ (cat.)} H_2S_3 + 2MePh_2SiOCOCF_3$$

In contrast to the known method[9] a more polar solvent (trichloromethane instead of benzene) was used. A further acceleration of the reaction was achieved by adding an approximately equimolar amount of water dissolved in the trifluoroacetic acid.

After complete removal of the solvent, water, and excess CF_3COOH the H_2S_3 was isolated by vacuum distillation. The course of the reaction and the purity of the sample were checked by NMR spectroscopy. The sample contained more than 90% H_2S_3 while H_2S, H_2S_2, and H_2S_4 comprised the remainder.

3. Observed Spectra

Pure Rotational Spectrum. One of the main obstacles toward detecting spectral lines of *trans*-H_2S_3 is their low intensity resulting from the expected small permanent electric dipole moment of the molecule. Our ab initio calculations reveal (section 4, see also ref 10) that the main contributions to the permanent electric dipole moment arise from the SH bonds. In the case of the *cis* conformation, the two SH dipole moments add and a relatively large dipole moment along the c-axis results. For the *trans* form, the SH bond dipole moments partially cancel because of C_2 symmetry thus leading to a rather small electric dipole moment along the b-axis, which coincides with the C_2-axis of *trans*-H_2S_3 (Figure 1). The presence of a C_2 symmetry axis has important consequences on the statistical weights of the energy levels and thus on the relative intensities of rotational lines. Just as in the case of H_2S_2[11] one expects a 3:1 intensity alternation for the *trans* form for all those high J-transitions whose K-degeneracy can be

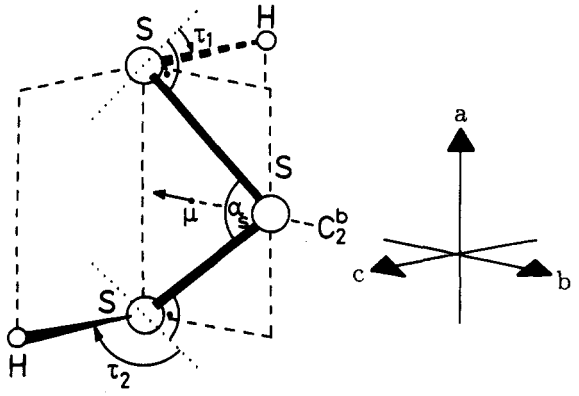

Figure 1. Structure of *trans*-H_2S_3 and orientation of principal axes of inertia. The C_2 symmetry axis is aligned with the *b*-principal axis.

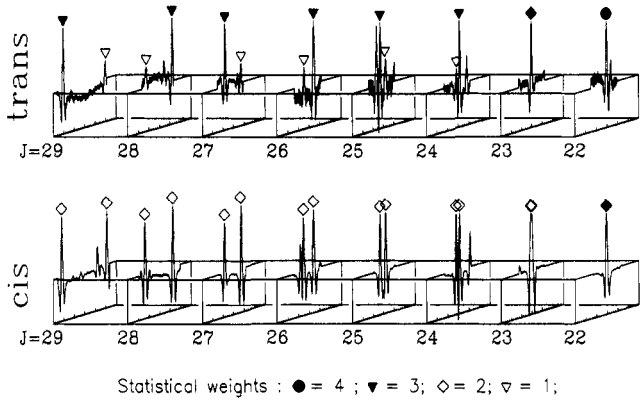

Figure 2. Recorded $^rQ_7$-branch of *trans*-H_2S_3 and *cis*-H_2S_3. The range of the *J* values ($22 \leq J \leq 29$) displays the onset of the asymmetry splitting with the characteristic intensity patterns which allow detection of the two conformations: The *b*-type lines of C_2-symmetrical *trans*-H_2S_3 display the typical 3:1 intensity pattern, whereas the *c*-type spectra of C_s-symmetrical *cis*-H_2S_3 do not show any intensity alternation. Each frequency scale amounts to 12 MHz.

resolved. It is this intensity alternation we searched for and which provides the main piece of evidence for establishing the existence of *trans*-H_2S_3.

The *trans* form **1** is a slightly asymmetric prolate rotor, with predicted rotational and centrifugal distortion constants rather similar to those of *cis* form **2**. The most conspicuous fingerprints of perpendicular spectra of near prolate tops are the compactness of the *Q*-branch *J*-pattern of the individual rotational lines. As in the case of the assignment of *cis*-H_2S_3[4] and its vibrationally excited states,[7] we searched for further *Q*-branch structures associated with the *trans* form and possibly interwoven with the ground state *Q*-branches of *cis*-H_2S_3. In addition to the already known positions of the vibrational ground- and excited-state *Q*-branch heads of the *cis* conformer[4,5,7] the present high sensitivity frequency search revealed additional *Q*-branches. These newly discovered relatively low intensity *Q*-branch heads appeared in a very closely equidistant pattern positioned always toward lower frequencies of the highly intense ground-state *Q*-branches of the *cis* conformer. The *trans* conformer has been assigned as the carrier of these spectra. Unequivocal evidence for this assignment stems from the fact that individual *J* lines of a candidate *Q*-branch if followed toward high *J* values start to split into doublets whose components show the typical $3{:}1 = (I+1)/I$ nuclear spin intensity alternation. For asymmetric rotors Fermi–Dirac spin statistics are only obeyed if identical nuclei with half-integral spin—here hydrogen nuclei with $I = {}^1/_2$—are exchanged by a rotation by π at a C_2 symmetry axis. For *trans*-H_2S_3 the *b*-principal axis is also the symmetry axis. As an illustrative example we show in Figure 2 high *J* rotational lines ($J \geq 22$) of the $^rQ_7$-branch at 172 GHz, which exhibit the onset of the *K*-splitting and thus the expected intensity alternation. Only for a narrow range of *J*

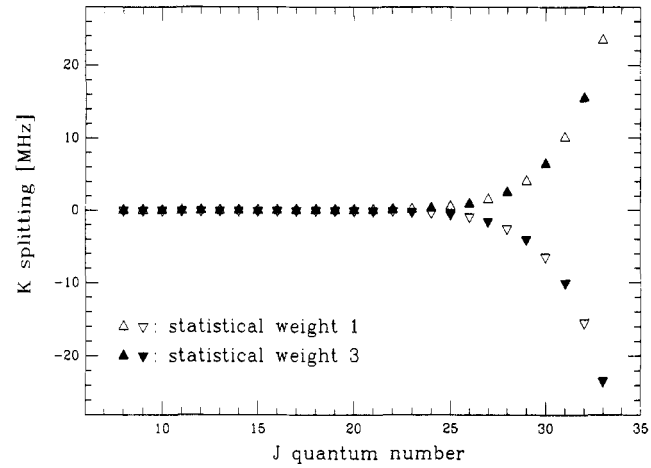

Figure 3. *K*-splitting of the $^rQ_7$-branch; △ ▲, upper component; ▽ ▼, lower frequency component.

values can the intensity alternation be easily perceived: for high *J* values ($J \geq 30$) the *K*-splitting is too large to be easily recognizable whereas for low *J* values ($J \leq 23$) the lines show no detectable splitting. In the low *J* case the intensity alternation of *trans*-H_2S_3 is not observed because lines with the two different nuclear statistical weights coincide and thus all low *J* lines, which are necessary for locating the origin of the *Q*-branch, do not reveal the C_2 symmetry of the molecule at first sight. This fact is depicted in Figure 3, which shows the *K*-splitting dependence on the *J* quantum number together with the associated nuclear statistical weight. In passing, it ought to be noted that aside from the rather different intensity at low *J* values, the *Q*-branches of *cis*- and *trans*-H_2S_3 are very similar in their pattern and not easily discernible. In fact the patterns of vibrationally excited *cis*-H_2S_3 or ground-state *cis*-$H^{34}SSSH$ spectra display a deceptively close resemblance with that of ground-state *trans*-H_2S_3 in those parts where no asymmetry splitting is observable.

The *b*-component of the dipole moment does not vanish in *cis*-H_2S_3, but it is expected to be very small. Considering the structural similarities of *cis*- and *trans*-H_2S_3 we can safely estimate the magnitude of μ_b of the *cis* conformer to be almost equal to the dipole moment of the *trans* form, where only the *b*-component exists by symmetry. The line positions of the *b*-type transitions of *cis*-H_2S_3 can be predicted very accurately, since we know the molecular parameters.[5] The search for those weak transitions was also successful, and will be published elsewhere. In addition to the *Q*-branch transitions of the *trans* form, we have identified about 100 *R*-branch and several *P*-branch transitions of *trans*-H_2S_3. By fitting these data with Watson's effective Hamiltonian (S-reduced), we have determined the rotational and centrifugal distortion constants very accurately. The complete analysis of the rotational spectrum of *trans*-H_2S_3 will be published elsewhere.

Infrared Fourier Transform Spectrum. Figure 4 shows three parts of the recorded infrared spectrum. According to the assignments of the liquid phase spectra[6] and on the assumption of the similarity of the vibrational frequencies of *cis*- and *trans*-H_2S_3, we have identified the absorption bands as follows:

The absorption centered at 485 cm^{-1} should be a complex of the SS stretching bands. From the molecular structure, we expect here for both rotamers, a *b*- and/or a *c*-type (symmetric SS stretch) and an *a*-type (antisymmetric SS-stretch) band. Although the observed spectrum, Figure 4a, indicates no intense central *Q*-branch of an *a*-type band, the ab initio calculations, as shown below, suggest strongly that the absorptions are contributed by the antisymmetric SS-stretch bands of both rotamers.

The absorption centered at 860 cm^{-1} should result from the HSS-bending bands. We expect for both rotamers, a *b*- and/or *c*-type (symmetric HSS bend) and an *a*-type (antisymmetric HSS bend) band. We tentatively assign the two sharp absorptions at

TABLE I: Observed Millimeter Wave Transitions of the $^rQ_7$-Branch of *trans*-H_2S_3 (*b*-type) in MHz[a]

J'	K_a'	K_c'	J''	K_a''	K_c''	measured	o-c
8	8		8	7		172 839.958	0.020
9	8		9	7		172 837.508	0.015
10	8		10	7		172 833.326	0.011
11	8		11	7		172 826.953	0.010
12	8		12	7		172 817.860	-0.008
13	8		13	7		172 805.537	0.001
14	8		14	7		172 789.350	0.006
15	8		15	7		172 768.627	-0.016
16	8	8	16	7	9	172 742.728	-0.005
16	8	9	16	7	10	172 742.728	-0.006
17	8	9	17	7	10	172 710.850	-0.016
17	8	10	17	7	11	172 710.850	-0.020
18	8	11	18	7	12	172 672.252	-0.002
18	8	10	18	7	11	172 672.252	0.009
19	8	12	19	7	13	172 626.024	-0.011
19	8	11	19	7	12	172 626.024	0.011
20	8	13	20	7	14	172 571.299	-0.014
20	8	12	20	7	13	172 571.299	0.032
21	8	14	21	7	15	172 507.057	-0.075
21	8	13	21	7	14	172 507.057	0.015
22	8	15	22	7	16	172 432.466	-0.018
22	8	14	22	7	15	172 432.466	0.157
23	8	16	23	7	17	172 345.984	-0.317
23	8	15	23	7	16	172 345.984	0.008
24	8	17	24	7	18	172 247.458	-0.005
24	8	16	24	7	17	172 246.800	-0.074
25	8	18	25	7	19	172 134.792	-0.001
25	8	17	25	7	18	172 133.761	0.008
26	8	19	26	7	20	172 007.043	-0.017
26	8	18	26	7	19	172 005.258	-0.010
27	8	20	27	7	21	171 863.020	0.037
27	8	19	27	7	20	171 859.984	0.020
28	8	21	28	7	22	171 701.241	0.002
28	8	20	28	7	21	171 696.268	0.012
29	8	22	29	7	23	171 520.453	-0.016
29	8	21	29	7	22	171 512.418	0.016
30	8	23	30	7	24	171 319.296	-0.002
30	8	22	30	7	23	171 306.463	-0.005

[a] The frequency accuracy for not overlapped lines is better than 30 kHz.

TABLE II: Observed Millimeter Wave Transitions of the $^rQ_8$-Branch of *cis*-H_2S_3 (*c*-type) in MHz[a]

J'	K_a'	K_c'	J''	K_a''	K_c''	measured	o-c
8	8		8	7		172 869.797	0.042
9	8		9	7		172 867.328	0.033
10	8		10	7		172 863.047	-0.042
11	8		11	7		172 856.656	-0.023
12	8		12	7		172 847.594	0.018
13	8		13	7		172 835.203	0.011
14	8		14	7		172 818.938	-0.008
15	8		15	7		172 798.125	-0.005
16	8	8	16	7	10	172 772.172	-0.016
16	8	9	16	7	9	172 772.172	-0.014
17	8	9	17	7	11	172 740.234	-0.003
17	8	10	17	7	10	172 740.234	0.002
18	8	10	18	7	12	172 701.500	-0.016
18	8	11	18	7	11	172 701.500	-0.005
19	8	11	19	7	13	172 655.172	0.004
19	8	12	19	7	12	172 655.172	0.027
20	8	12	20	7	14	172 600.297	-0.002
20	8	13	20	7	13	172 600.297	0.045
21	8	13	21	7	15	172 535.891	-0.052
21	8	14	21	7	14	172 535.891	0.043
22	8	14	22	7	16	172 461.000	-0.104
22	8	15	22	7	15	172 461.000	0.079
23	8	15	23	7	17	172 374.516	-0.187
23	8	16	23	7	16	172 374.516	0.155
24	8	16	24	7	18	172 275.609	-0.014
24	8	17	24	7	17	172 274.984	-0.022
25	8	17	25	7	19	172 162.672	-0.015
25	8	18	25	7	18	172 161.563	-0.020
26	8	18	26	7	20	172 034.625	-0.038
26	8	19	26	7	19	172 032.734	-0.025
27	8	19	27	7	21	171 890.266	-0.011
27	8	20	27	7	20	171 887.063	0.003
28	8	20	28	7	22	171 728.188	-0.022
28	8	21	28	7	21	171 722.859	-0.005
29	8	21	29	7	23	171 547.125	-0.004
29	8	22	29	7	22	171 538.422	-0.008
30	8	22	30	7	24	171 345.688	0.006
30	8	23	30	7	23	171 331.750	-0.019

[a] The frequency accuracy for not overlapped lines is better than 30 kHz.

860 and 863 cm^{-1} to be the *a*-type *Q*-branch of *cis*- and *trans*-H_2S_3, respectively. The ab initio calculations discussed in the next section suggest that the stronger one should result from the *trans* form and the weaker one from the *cis* form.

The absorption centered at 2545 cm^{-1} can be assigned to the SH-stretching bands. The antisymmetric SH-stretching mode of *trans*-H_2S_3 and the symmetric SH-stretching mode of the *cis* conformer should dominate the spectrum. They both are *c*-type bands and the *Q*-branch-like central absorptions are expected. For a more detailed analysis of the infrared spectra of H_2S_3, measurements with much higher resolution are required.

4. Ab Initio Calculations

All ab initio calculations have been carried out with the (12s9p1d)[621111,52111,1] basis set of McLean and Chandler (MC)[12] adding the *H* functions from Pople's 6-311G(d,p) basis set.[13] The resulting basis set has valence TZ+P quality and we use for it the abbreviation MC-311G(d,p). Both perturbation and coupled cluster (CC) theory have been applied to obtain correlation corrected geometries and energies for **1** and **2**. Perturbation theory calculations have been done at second order using the Møller–Plesset perturbation operator (MP2).[14] This level of theory is known to provide reasonable correlation corrections resulting from all double (D) excitations. More accurate data are provided by CC methods since they contain infinite order effects. As an economically attractive CC method, we have employed quadratic CI (QCI) with all singles (S) and D excitations (QCISD) utilizing the analytical QCISD gradients by Gauss and Cremer for the geometry optimizations.[16] Thus, the two levels of theory employed are MP2/MC-311G(d,p) and QCISD/MC-31G(d,p). Since the two methods are applied to closely related conformers, we can expect that QCI relative energies will be accurate to 0.1 kcal/mol, bond lengths to 0.005 Å, bond angles to 0.5°, dihedral angles to 1.5°, and dipole moments to 0.1 D.

In Figure 5, MP2/MC-311G(d,p) (in normal print) and QCISD/MC-311G(d,p) (in italics) geometries, energies, and dipole moments are summarized. Both MP2 and QCISD predict that **1** is more stable by 0.27 and 0.22 kcal/mol, respectively, than **2**, thus confirming earlier HF results[3] and a variety of semiempirical and force field calculations.[17] The zero-point energies of **1** and **2** (13.15 and 13.17 kcal/mol) and other vibrational corrections differ only marginally, which means that our best estimate of the enthalpy difference between the two forms is 0.25 kcal/mol in favor of **1**.

In view of the small energy difference it is not surprising that the geometries of the two conformers are almost identical (Figure 5). The SS (SH) bonds are somewhat longer (shorter) than those observed for HSSH (2.0564 and 1.3421 Å[11]) while the SSH angles are almost identical with those of HSSH (97.88°). The dihedral angles are close to 86° (*trans* conformer) and 89° (*cis* form), comparable to the value of HSSH (90.34°). These data are in line with enhanced lone pair–lone pair interactions in H_2S_3 compared to those in HSSH and the fact that anomeric stabilization, which leads to shortening of the SS bonds, is only possible for the electron lone pairs of the central S atom. The anomeric delocalization of electron lone pairs at the terminal S atoms leads to lengthening of the vicinal SS bonds and, therefore, is responsible for the increase in SS bond lengths when going

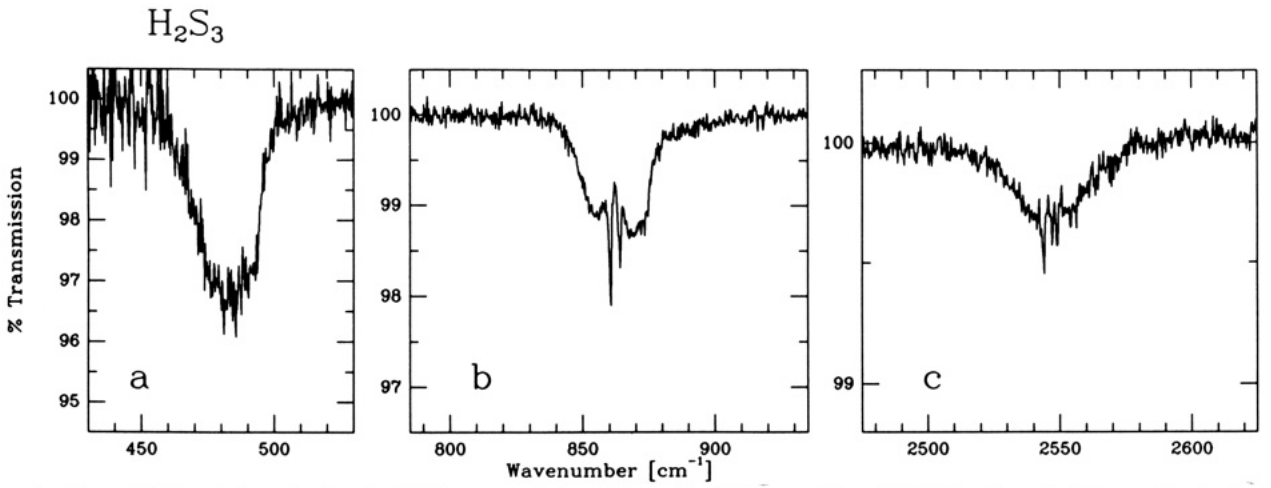

Figure 4. Observed infrared absorption bands of H_2S_3 at a resolution of 0.5 cm^{-1}: (a) SS stretching; (b) HSS bending; (c) SH stretching bands. For details see text.

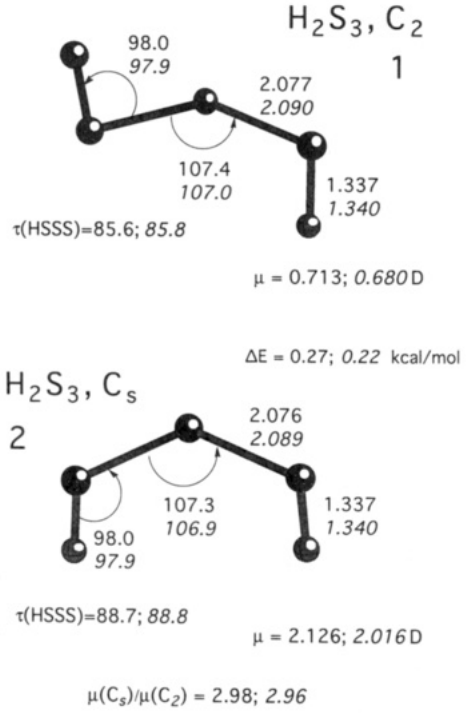

Figure 5. Ab initio geometries, energies, and dipole moments of *trans*- and *cis*-H_2S_3: MP2/TZ+P values in normal print; QCISD/TZ+P values in italics. Bond lengths are given in Å, bond angles and dihedral angles τ in deg, relative energies in kcal/mol, dipole moments in debye. The absolute values of calculated energies are −1194.51511 (**1**, MP2/TZ+P) and −1194.55619 (**1**, QCISD/TZ+P).

from H_2S_2 to H_2S_3. If anomeric delocalization effects are not possible, as in the planar forms **3**–**5**, the SS bonds are considerably longer than in **1** and **2**. We conclude that both *trans* and *cis* forms are stabilized by staggering of electron lone pairs at the S atoms and by anomeric delocalization of electron lone pairs of the S atoms.

As discussed in the case of H_2O_3,[1] the energy difference between the two conformers results from XH (X = O, S) bond dipole interactions. In the case of the C_2 form the XH bond dipoles are antiparallel but shifted to different sides of the XXX plane. Therefore, their interaction should lead to some weak stabilization, possibly cancelled by electrostatic repulsion of the negatively charged terminal X atoms. In the case of the C_s form, the XH bond dipoles are parallel and, therefore, repel each other which leads to destabilization of the C_s form. Accordingly, the C_s form of H_2O_3 has been found to be 3.5 kcal/mol less stable than the corresponding C_2 form.[1]

In the case of H_2S_3, interactions between the bond dipoles are much weaker for two reasons: First, the bond dipole moments are rather small, which is clearly reflected by the calculated small gross atomic charges (see Table III). The latter indicate that the electronegativities of H (2.2) and S(2.5) are comparable in magnitude giving S a somewhat stronger electron withdrawing ability. Secondly, the distance between the bond dipoles (3.4 Å) is about 1 Å larger than in the case of H_2O_3. Since dipole–dipole interaction energies are proportional to $1/r^3$, one can estimate that just because of the larger r value the interaction energy for the SH bond dipoles should be smaller by a factor of 3.

Because of the weak SH–SH interactions and because of the fact that all other electronic effects (lone pair–lone pair repulsion, anomeric lone pair delocalization) are almost identical, relative energies for the two forms are similar with a 0.2 kcal/mol advantage for the *trans* form **1**.

Spectroscopic Identification of 1 and 2. Since both conformations do not differ very much with regard to energy and geometry, it remains to be clarified by which properties **1** and **2** can be distinguished. From our calculations we predict that this is best done by (a) rotational constants, (b) molecular dipole moments, and (c) infrared spectra. A prerequisite for utilizing these properties and differentiating between *cis* and *trans* conformer is the high spectral resolution offered by microwave spectroscopy.

As shown in Table III rotational constants A, B, and C are between 1 and 11 MHz larger for the C_s form **2** than for the C_2 form **1**, which is a direct consequence of the parallel alignment of the SH bonds in the *cis* form. Even if one considers that the calculated rotational constants are seldom more accurate than a couple of MHz and often deviate by 300–400 MHz, trends seem to be correctly predicted by ab initio calculations. Distinction between **1** and **2** is possible using measured rotational constants. However, the final spectroscopic identification is only secured by the detection of the 3:1 intensity alternation of the conformer possessing a C_2 symmetry axis, i.e., **1**.

Calculated HF and MP2 dipole moments are often 5 to 10% too large while CC values can be accurate within a few percent. Hence, the QCISD/MC-311G(d,p) values of 0.680 and 2.016 D (Figure 5 and Table III) represent our most accurate predictions for the dipole moments of **1** and **2**. In the *trans* form, there is only a *b*-component (Table III) which at both levels of theory is almost identical with the *b*-component of the *cis* form, thus confirming the predictions made above. Clearly, the calculated dipole moments can also supply information for the identification of the two conformations.

In Figure 6, MP2/MC-311G(d,p) infrared spectra are shown for the two conformations. An analysis of the spectra in terms of vibrational frequencies, intensities, isotopic shifts, and mode

TABLE III: Experimental and Calculated Properties of HSSSH

A. Rotational Constants [MHz]

conformation	method	*A*	*B*	*C*
1, C_2	expt	14 098.89744(42)	2750.15137(15)	2371.69779(14)
	MP2	13 904	2675	2313
	QCISD	13 636	2656	2292
2, C_s	expt	14 103.20962(25)	2752.75945(11)	2373.86989(12)
	MP2	13 915	2676	2314
	QCISD	13 646	2657	2293

B. Atomic Charges [melectron]

		S_C[a]	S_T[a]	H
1, C_2	MP2	−46	−50	+73
	QCISD	−46	−38	+61
2, C_s	MP2	−48	−42	+66
	QCISD	−48	−30	+54

C. Dipole Moments [Debye]

		a	*b*	*c*	total
1, C_2	MP2	0	−0.713	0	0.713
	QCISD	0	−0.680	0	0.680
2, C_s	MP2	0	−0.717	−2.001	2.126
	QCISD	0	−0.685	−1.897	2.016

[a] S_C and S_T denote central and terminal S atom.

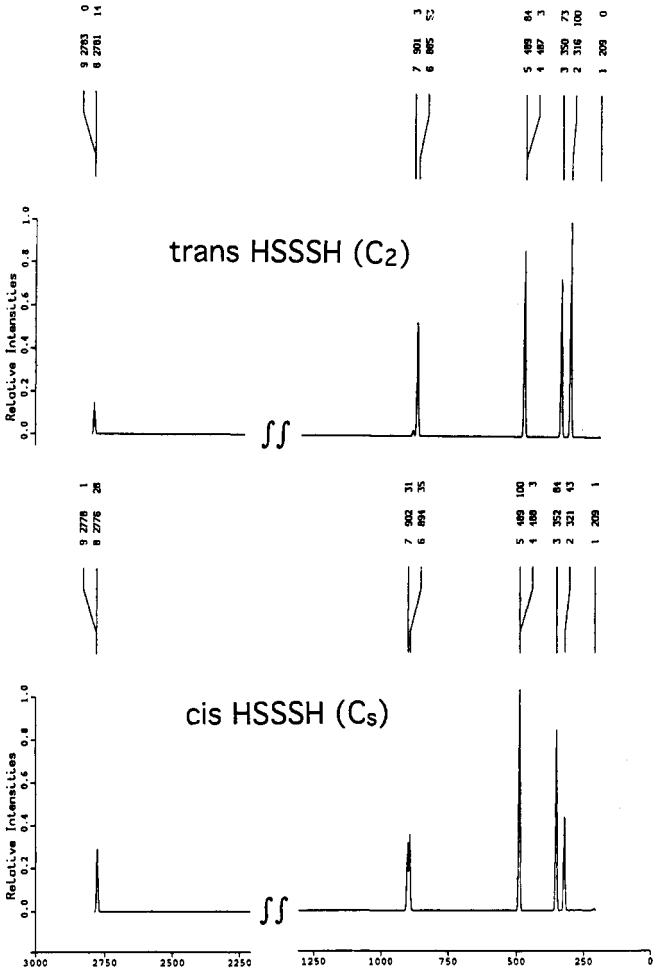

Figure 6. MP2/MC-311G(d,p) infrared spectra of *trans*- and *cis*-H_2S_3. Frequencies (in cm^{-1}) and intensities (relative to the most intense band) are given above each band. The numbering of the bands complies with that given in Table IV.

assignments is given in Table IV. Since the vibrational frequencies have been calculated within an harmonic approximation, the SH stretching frequencies will be about 9% too large while the lower

TABLE IV: Unscaled MP2/MC-311g(d,p) Frequencies and Intensities[a]

		H_2S_3, C_2[b]		D_2S_3, C_2		
no.	assignment	ω	(*I*)	ω	(*I*)	shift
9	SH sym stretch	2783	(0.1)	1999	(0.0)	−784
8	SH antisym stretch	2781	(4.1)	1998	(2.2)	−783
7	SSH sym bend	901	(0.7)	649	(0.4)	−251
6	SSH antisym bend	885	(15.2)	645	(8.8)	−240
5	SS antisym stretch	489	(24.1)	448	(24.6)	−1
4	SS sym stretch	487	(0.9)	487	(0.9)	0
3	antisym torsion	350	(21.1)	259	(10.8)	−91
2	sym torsion	316	(28.8)	237	(13.7)	−79
1	SSS bend	209	(0.0)	197	(1.7)	−12
		H_2S_3, C_s[c]		D_2S_3, C_s		
no.	assignment	ω	(*I*)	ω	(*I*)	shift
8	SH sym stretch	2776	(7.4)	1994	(4.0)	−782
9	SH antisym stretch	2778	(0.3)	1996	(0.0)	−782
7	SSH sym bend	902	(8.2)	658	(4.5)	−244
6	SSH antisym bend	894	(9.2)	643	(4.9)	−251
5	SS antisym stretch	489	(26.3)	489	(25.2)	0
4	SS sym stretch	488	(0.8)	487	(0.8)	−1
3	antisym torsion	321	(11.4)	231	(5.9)	−90
2	sym torsion	351	(22.0)	263	(10.3)	−88
1	SSS bend	209	(0.2)	203	(0.1)	−6

[a] Wavenumbers in [cm^{-1}], intensities in [km/mol]. [b] Experimental frequencies from liquid IR[6] are: ω_9, 2540; ω_8, 2532; ω_7, 868; ω_6, 856; ω_5, 477; ω_4, 487. Gas phase IR (this work): ω_8, 2542; ω_6, 860; ω_5, 480 cm^{-1}. [c] Experimental frequencies from gas phase IR (this work) are: ω_8, 2548; ω_6, 865; ω_5, 480 cm^{-1}.

frequency values should be closer to experimental values because of a fortuitous cancellation of errors.

The calculated vibrational frequencies reveal that despite somewhat different intensities neither SH stretch, SS stretch, SSS bend, nor the two torsional modes should provide a basis for a clear distinction between **1** and **2** since the corresponding infrared bands overlap or have intensities too low to be observed. The only exception is the SSH bending mode at 900 cm^{-1}. In the case of **1**, the antisymmetrical SSH bending mode is strong while the symmetrical SSH bending mode is very weak. However, for **2** the SSH bending modes lead to two somewhat less intense bands which are shifted to somewhat higher wavenumbers. Thus, if both conformers are present, they should be identified by the three bands resulting from the SSH bending modes. The same is also true for the infrared bands of C_2 and C_s symmetrical DSSSD, which apart from the DSS bending modes do not provide a basis for identification of the two conformations.

Kinetic Stability of 1 and 2. Minimum energy rotations at the OO bonds of H_2O_3 follow a stepwise mechanism that has been coined a flip-flop rotation:[1] First, one OH group rotates into and through the OOO plane until the C_s form is reached with form **6** (Chart II) as the rotational transition state; then, the second OH group rotates in the opposite direction until the molecule adopts a new C_2 form. This flip-flop process seems to be typical for many geminal double rotors.[1] Furthermore, ring pseudorotation can be explained as a coupling of partial flip-flop processes.[1] Test calculations reveal that H_2S_3 undergoes the same rotational processes as H_2O_3. At the MP2/MC-311G(d,p) level, the rotational barrier for the interconversion of **1** into **2** is 8.3 kcal/mol (for the transition state geometry **6**, see Figure 7), i.e. both conformations are kinetically stable on the time scale of an infrared or millimeter wave spectroscopic investigation. However, a rotational barrier of 8.3 kcal/mol is not high enough to prevent a thermodynamic equilibrium between **1** and **2** in the gas phase at the temperatures of measurement. This means that independent of the conformation that has been predominantly formed in the synthesis of H_2S_3 (probably **2** because of its larger dipole moment and the larger solvation energy in polar solvents), at room temperature the ratio of **1** to **2** will be about 60:40.

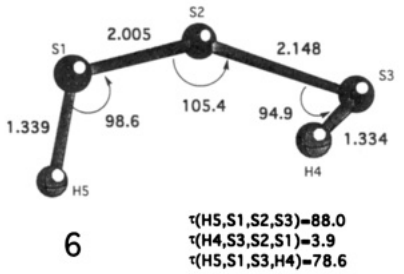

6

Figure 7. MP2/TZ+P geometry of the transition state of the flip-flop rotation leading from *trans*- to *cis*-H_2S_3. The transition state corresponds to form **6** of Chart II.

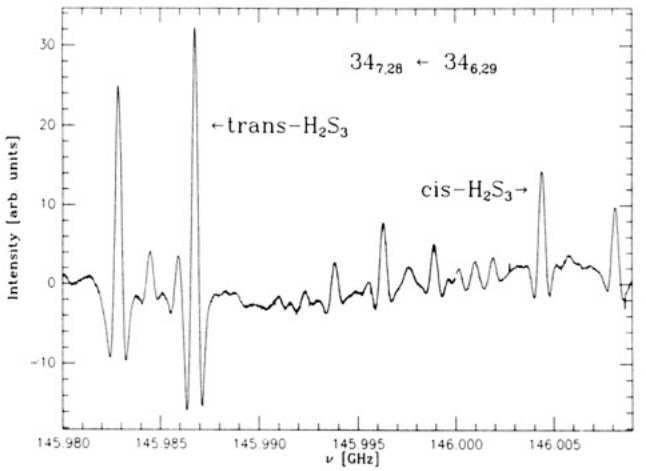

Figure 8. The $34_{7,28} \leftarrow 34_{6,29}$ transition of *cis*- and *trans*-H_2S_3, the frequency positions of which are accidentally very close.

5. Discussion

A comparison of the line intensities of the $^rQ_6$-branch lines between equal J-quantum numbers of *cis*-H_2S_3 (*b*-type) and of the *trans* form reveals that both conformers must have about the same abundance. Our ab initio calculations predict that **2** is 0.25 kcal/mol (87 cm^{-1}) higher in energy than **1**. Taking this energy difference into account, one obtains for the abundance ratio at room temperature $n_{cis}/n_{trans} \approx 0.66$, which matches the experimentally determined value of 0.58(10) obtained from Figure 8. The latter value is based on the nuclear statistical weights and on the ab initio result that $\mu_b(cis) \approx \mu(trans)$. Fortunately, the distance of the shown Q-branch transitions $J = 34_{7,28} \leftarrow 34_{6,29}$ of *cis*- (*b*-type) and *trans*-H_2S_3 is only 18 MHz (Figure 8); therefore the line intensity ratios could be determined accurately enough to confirm an energy difference of 0.32(10) kcal/mol between *trans* and *cis* conformer at room temperature. This value is also predicted on the basis of the transitions of $J = 33_{7,27} \leftarrow 33_{6,28}$, the frequency distance of which is also 18 MHz.

In addition, the ratio of the calculated electric dipole moments $\mu(cis) = 2.02$ D and $\mu(trans) = 0.68$ D (Table III) could be checked by the spectrum shown in Figure 9, where the same $^rQ_6$ ($J = 24$) lines for *cis*- (*c*-type) and *trans*-H_2S_3 are displayed simultaneously. With $\mu_b(cis) \approx \mu(trans)$ (Table III), the nuclear statistical weights, and an abundance ratio of 0.58 at room temperature, one obtains the experimental ratio $\mu_c(cis)/\mu(trans) = 2.7(0.7)$, which compares well with the corresponding QCISD ratio of 2.96 (Figure 5).

Our results show that the conformational preferences of H_2S_3 differ from those of H_2O_3 in so far as energetically the formation of helix form and crown form are both possible with a slight preference for the former. This seems to be in connection with the well-known tendency of sulfur to form both chains of S atoms and rings of S atoms. Further investigations of higher polysulfanes must be carried out to verify this prediction.

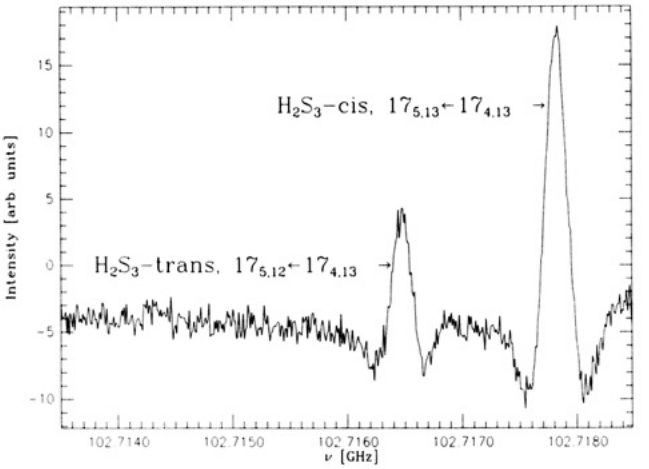

Figure 9. The $17_{5,13} \leftarrow 17_{4,13}$ transition of *cis*-H_2S_3 is accidentally close to the $17_{5,12} \leftarrow 17_{4,13}$ transition of *trans*-H_2S_3; both transitions share a common lower level.

Acknowledgment. Work at Köln was supported in part by the Deutsche Forschungsgemeinschaft via Research Grant SFB 301. Work at Göteborg was supported by the Swedish Natural Science Research Council (NFR) and the Nationellt Superdatorcentrum (NSC), Linköping, Sweden. S.D. gratefully acknowledges financial support from the DFG during his stay at the Universität zu Köln.

References and Notes

(1) Cremer, D. *J. Chem. Phys.* **1978**, *69*, 4456.
(2) The terms *trans* and *cis* are used for geometrical isomers that can only be interconverted by breaking a bond. Therefore, their use in the case of conformers is not correct. Nevertheless, we stick to these terms for reasons of convenience and since they have been previously used in the literature.[17]
(3) Cremer, D.; Gauss, J. Unpublished results.
(4) Mauer D.; Winnewisser, G.; Yamada, K. M. T.; Hahn, J.; Reinartz, K. *Z. Naturforsch.* **1988**, *A43*, 617.
(5) Mauer, D.; Winnewisser, G.; Yamada, K. M. T. *J. Mol. Struct.* **1988**, *190*, 457.
(6) Wieser, H.; Krueger, P. J.; Muller, E.; Hyne, J. B. *Can. J. Chem.* **1969**, *47*, 1633.
(7) Mauer, D.; Winnewisser, G.; Yamada, K. M. T. *J. Mol. Spectrosc.* **1989**, *136*, 380.
(8) Liedtke, M.; Schieder, R.; Winnewisser, G. To be submitted for publication.
(9) Hahn, J.; Altenbach, K. *Z. Naturforsch.* **1986**, *41b*, 675.
(10) Meyer, B.; Peter, L.; Spizter, K. *Inorg. Chem.* **1977**, *16*, 27.
(11) Behrend, J.; Mittler, P.; Winnewisser, G.; Yamada, K. M. T. *J. Mol. Spectrosc.* **1991**, *150*, 99.
(12) McLean, A. D.; Chandler, G. S. *J. Chem. Phys.* **1980**, *72*, 5639.
(13) Krishnan, R.; Binkley, J. S.; Seeger, R.; Pople, J. A. *J. Chem. Phys.* **1980**, *72*, 650.
(14) (a) Møller, C.; Plesset, M. S. *Phys. Rev.* **1934**, *46*, 618. (b) Pople, J. A.; Binkley, J. S.; Seeger, R. *Int. J. Quantum Chem. Symp.* **1976**, *10*, 1.
(15) Pople, J. A.; Head-Gordon, M.; Raghavachari, K. *J. Chem. Phys.* **1987**, *87*, 5968.
(16) (a) Gauss, J.; Cremer, D. *Adv. Quantum Chem.* **1992**, *23*, 205. (b) Gauss, J.; Cremer, D. *Chem. Phys. Lett.* **1988**, *150*, 280.
(17) (a) Synder, J. P.; Harpp, D. N. *Tetrahedron Lett.* **1978**, *2*, 197. (b) For other calculations on H_2S_3, see refs 18 and 19.
(18) Trsic, M.; Laidlaw, W. G. *Int. J. Quant. Chem.* **1980**, *17*, 969.
(19) Laitinen, R.; Pakkanen, T. *J. Mol. Struct.* **1983**, *91*, 337.